Supporting Information

Biowaste Derived Porous Nano Carbon Supported Transition Metal Borides as an Efficient Electrocatalyst for Alkaline Water Splitting: A Waste to Wealth Approach

B Sirichandana, et al.,

Chemicals and reagents

Cobalt chloride hexahydrate ($CoCl_2 \cdot 6H_2O$), sodium borohydride ($NaBH_4$), and potassium hydroxide pellets (KOH) were sourced from Researchlab. Concentrated HCl was supplied by Thomas Baker, while ethanol was procured from Finar Chemicals. Nafion was procured from DTech Solutions, and Millipore water was employed as the general-purpose solvent.

Material Characterization

The morphological features and elemental composition were examined using energy-dispersive X-ray spectroscopy (EDS) and field emission scanning electron microscopy (FE-SEM) with a Thermo Scientific Apero 2S instrument. Transmission electron microscopy (TEM) imaging was conducted on a JEOL JEM-2010 system. X-ray diffraction (XRD) patterns were obtained using a Rigaku Miniflex 600 (Rigaku, Japan) with Cu-Kα radiation. Raman spectra were recorded on a Renishaw system (Horiba Model: LabRAM HR) employing a 532 nm laser source. The surface chemical states and atomic compositions were analyzed through X-ray photoelectron spectroscopy (XPS) on a Thermo ESCALAB 250XI. Fourier-transform infrared (FT-IR) spectra were measured using an IRSpirit-L spectrometer (SHIMADZU, Japan).

Electrochemical Measurements

For the electrochemical studies, a three-electrode system was used, consisting of a catalyst-deposited glassy carbon electrode (GCE, 3 mm, geometric surface area = 0.07 cm^2) as the working electrode, a saturated calomel electrode (SCE) as the reference electrode, and a graphite rod as the counter electrode. The catalyst ink was prepared by taking 5 mg of the synthesized catalyst powder

and 1mL of ethanol, followed by dispersion in an ultrasonic bath. The binder solution was prepared by mixing 40 µL Nafion (5 wt%) with 1 mL ethanol. A 10 µL of this binder solution was first drop-casted on the GCE, followed by successive drop-casting of 20 µL of catalyst ink, drying under an infrared lamp between each step. This process was repeated until a mass loading of 1.4 mg cm^{-2} was achieved. All electrochemical measurements were carried out using a potentiostat (CH16011E) from CH Instruments. 1M KOH was used as the electrolyte for all the electrochemical studies. Prior to HER measurements, surface conditioning was done by performing a chronoamperometry test until a steady current was obtained in order to ensure the removal of surface oxide. Linear Sweep Voltammograms (LSVs) were acquired at 10 mV/s scan rate in the potential range of -1.4 V to -1.06 V (vs. SCE) for HER. The potentials measured were converted to reversible hydrogen electrode (RHE) using the Nernst equation, $E = E_o + (0.059*pH)$ where E_o = 0.241 V. The electrochemical impedance spectroscopy (EIS) was performed in the frequency range of 100 kHz to 1 Hz to acquire charge transfer resistance (R_{ct}) and solution resistance (R_s) and the potential applied for HER was –0.29 V (vs. RHE). Polarization curves are presented with iR correction. Cyclic Voltammetry was carried out at different scan rates of 20, 40, 60, 80, 100, and 120 mV/sec in non-faradaic regions in order to obtain electrochemical surface area (ECSA) from double layer capacitance (C_{dl}). To C_{dl} values were obtained from the slope derived by performing a linear fit on the plot of the scan rates against the difference between cathodic and anodic current densities. The Tafel slope was determined by linear fitting of the plot of log current density versus overpotential.

The recyclability and stability of the catalyst were evaluated through 1000 LSV cycles and 40-hour chronoamperometric tests. During chronoamperometry, potential of –0.3 V (vs. RHE) was applied.

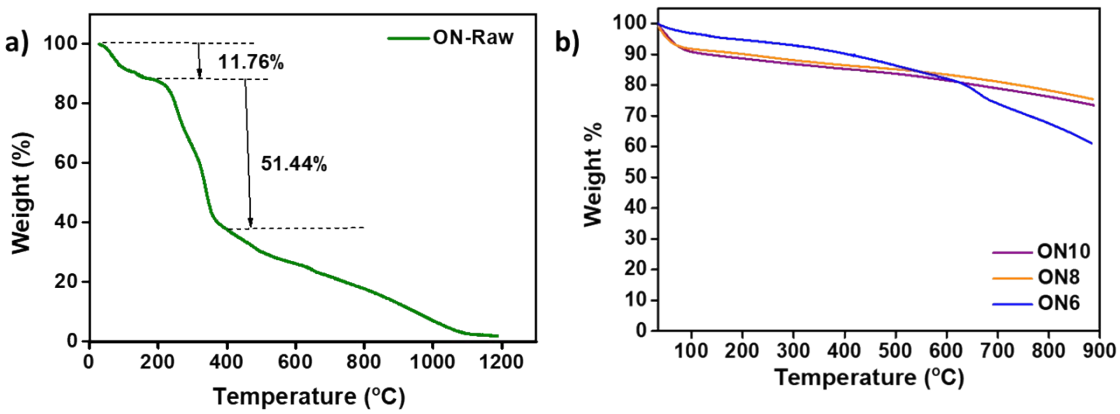

Fig S1. TGA plot of a) ON-Raw and b) ON10, ON8 and ON6

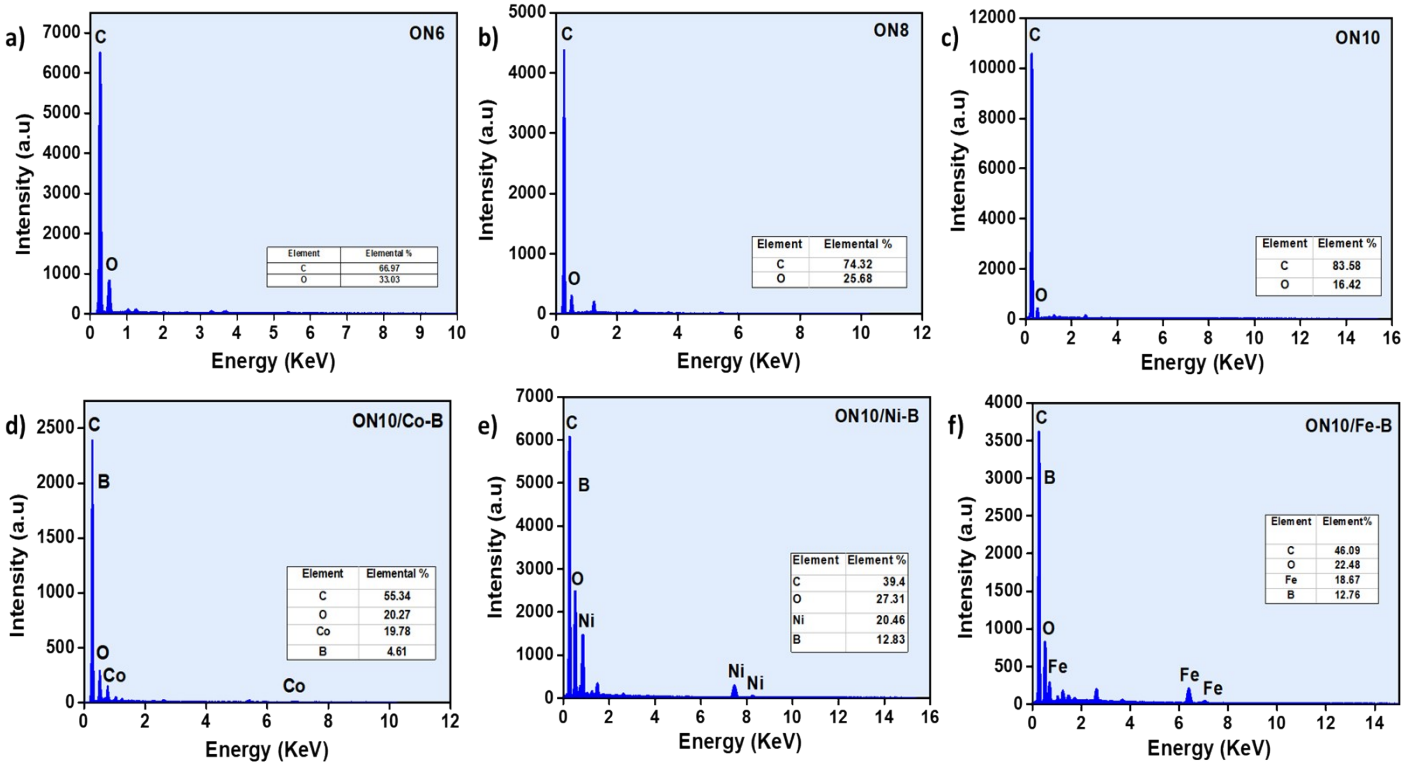

Fig S2. EDS image of a) ON6, b) ON8, c) ON10, d) ON10/Co-B, e) ON10/Ni-B, f) ON10/Fe-B

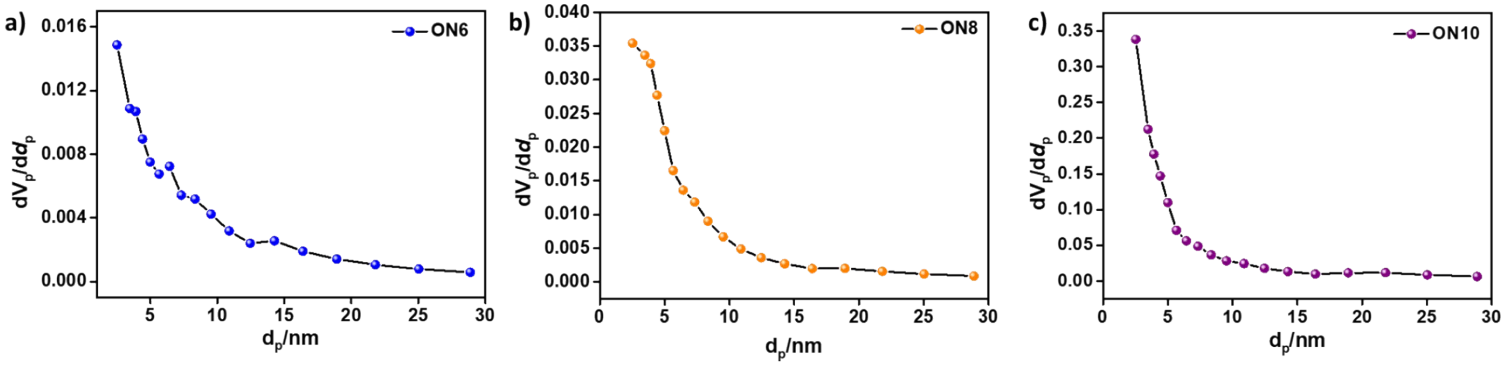

Fig S3. Pore size distribution of a) ON6, b) ON8 and c) ON10

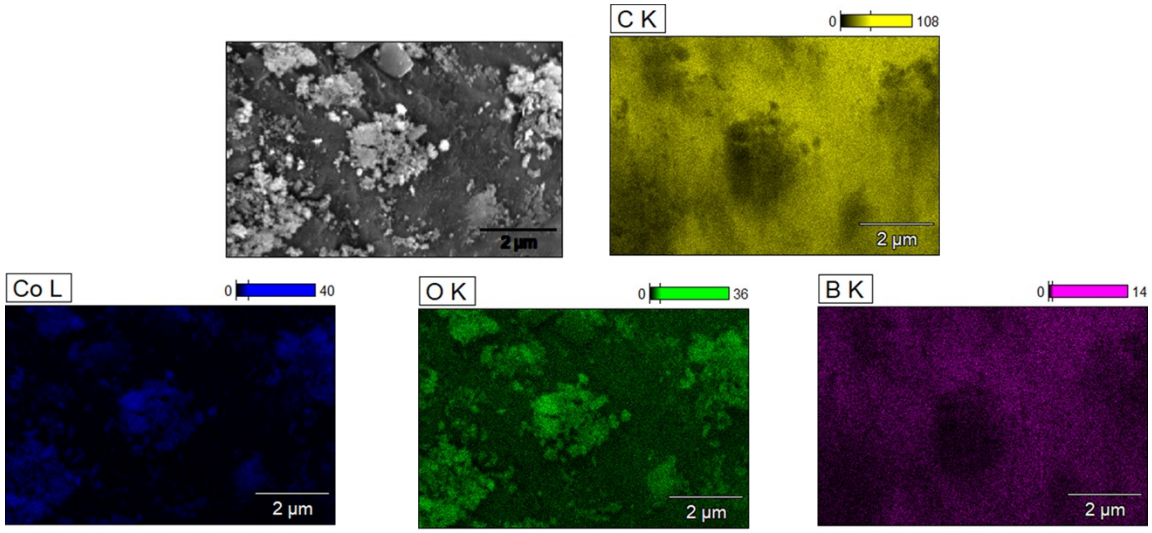

Fig S4. Elemental mapping of ON10/Co-B

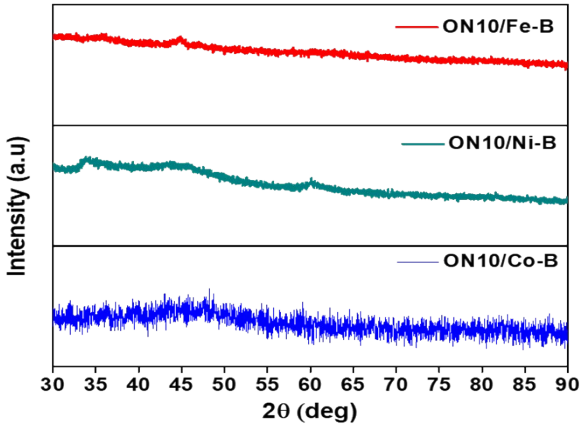

Fig S5. XRD pattern of ON10/Co-B, ON10/Ni-B and ON10/Fe-B

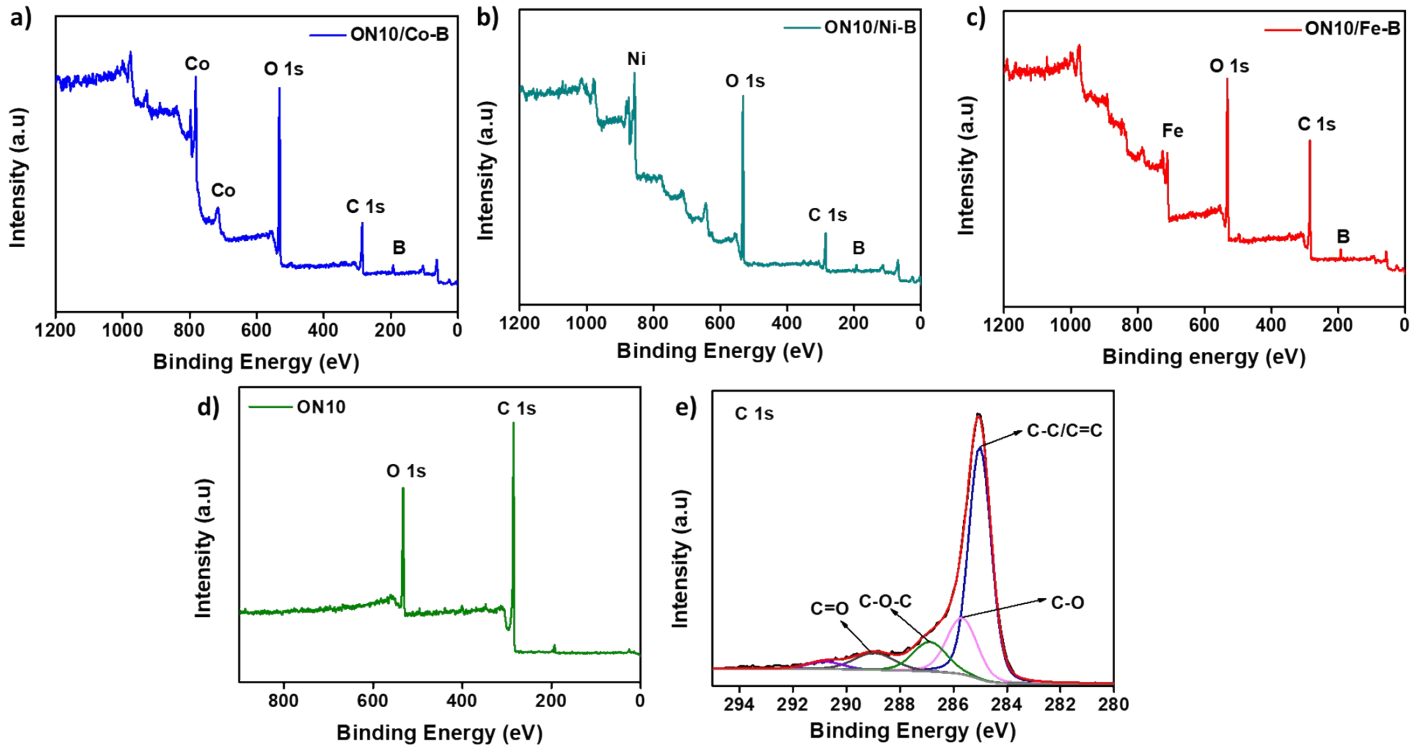

Fig S6. XPS survey spectra of a) ON10/Co-B b) ON10/Ni-B c) ON10/Fe-B d) ON 10 and e) C 1s XPS spectrum of ON10

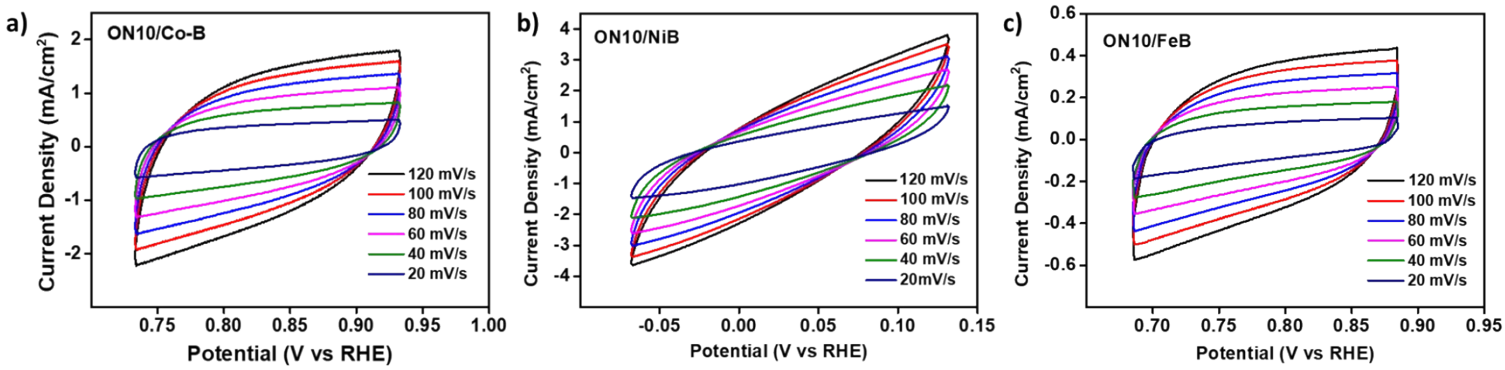

Fig S7. Cyclic voltammograms at different scan rates for a) ON10/Co-B b) ON10/Ni-B c) ON10/Fe-B in alkaline medium

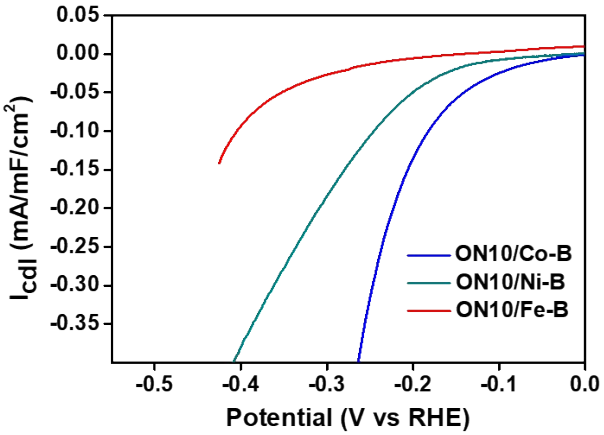

Fig S8. Plot of C_{dl} normalized current density against the applied potential for HER

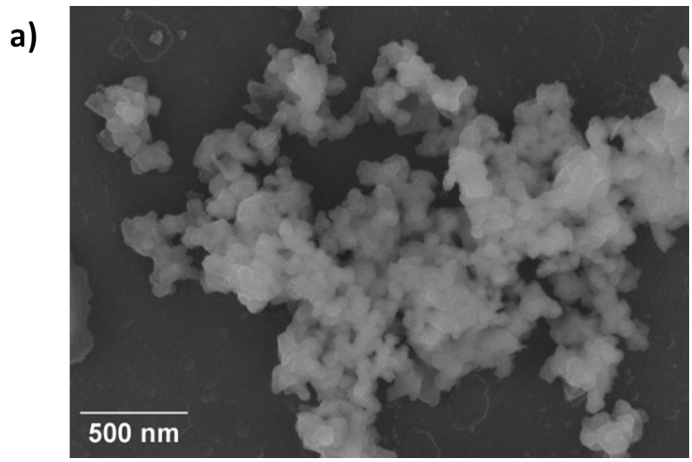

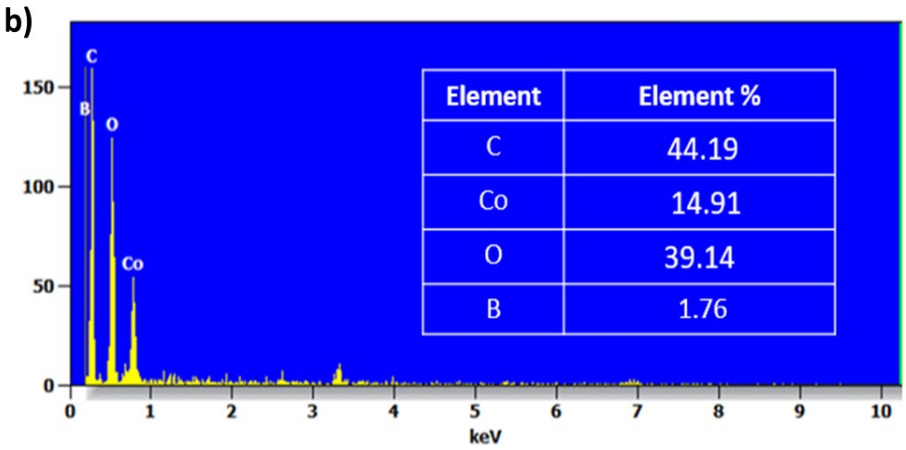

Fig S9. FESEM image of a) ON10/Co-B after HER, b) EDS of ON10/Co-B after HER

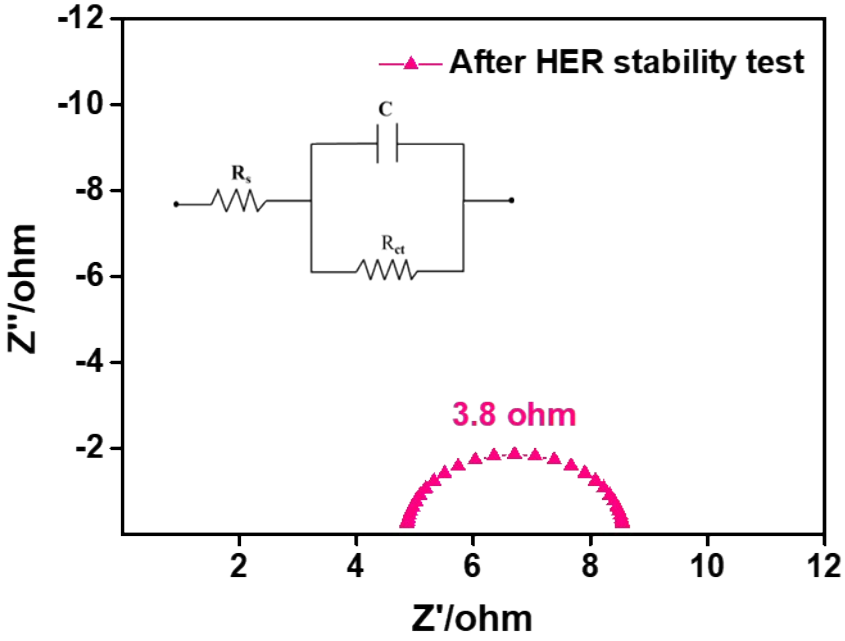

Fig S10. Nyquist plot for ON10/Co-B after HER stability test of 40h

Table 1. Comparative Analysis of η_{10} (10 mA/cm²), Electrolyte, Mass Loading, Substrate, iR compensation, Tafel Slope and Stability of ON10/Co-B Relative to Carbon- and Cobalt-Based Electrocatalysts Reported for HER [35-44]

Sl no	Catalyst	electrolyte	Mass loading (mg/cm²)	substrate	iR	η_{10} (mV)	Tafel slope (mV/dec)	stability	ref
1	Co/CoO@NC @CC	1M KOH	0.19	Carbon cloth	85%	-152	80	25h	35
2	CoS_2QDs@r GO	1M KOH	-	Glassy carbon electrode	-	-298	78	48h	36
3	Co@SCG-KU	1M NaOH	0.612	Glassy carbon electrode	-	-284	227.6	8h	37

4	Co_2P/Ni_2P/carbon nanotube (CNT)	1M KOH	0.2	Glassy carbon electrode	100 %	-202	57.95	48h	38
5	CoS_2/AC	1M KOH	-	Stainless steel	-	-378	134	10h	39
6	$MoS_2/Co_{1-x}S$@C	1M KOH	-	Nickel foam	-	-135	106	30h	40
7	Co@NGC-800	1M KOH	-	Nickel foam	No iR correction	-234	118	24h	41
8	$Co_{0.15}$@ARC	1M KOH	0.6	Carbon cloth	-	-172	108	20	42
9	Co@NC-A	1M KOH	1.5	Graphite disk	100 %	-162	158	50h	43
10	CoS_2/NiS_2@N-CNTs	1M KOH	-	Glassy carbon electrode	-	-126	71	12h	44
11	**ON10/Co-B**	**1M KOH**	**1.4**	**Glassy carbon electrode**	**100 %**	**-122**	**136**	**40**	**This work**